Scientific Research Publishing

World Journal of Engineering and Technology, 2023, 11, 113-135
https://www.scirp.org/journal/wjet
ISSN Online: 2331-4249
ISSN Print: 2331-4222

Numerical Study on Hydraulic Characteristics and Discharge Capacity of Modified Piano Key Weir with Various Inlet/Outlet Width Ratio

Ilan Ich[1,2], Genguang Zhang[1*], Anbin Li[1], Vinhteang Kaing[2,3], Ty Sok[2,4]

[1]College of Water Resources and Architectural Engineering, Northwest A&F University, Yangling, China
[2]Faculty of Hydrology and Water Resources Engineering, Institute of Technology of Cambodia, Russian Federation Blvd., Phnom Penh, Cambodia
[3]Department of Civil and Environmental Engineering, School of Environment and Society, Tokyo Institute of Technology, Tokyo, Japan
[4]Research and Innovation Center, Institute of Technology of Cambodia, Russian Federation Blvd., Phnom Penh, Cambodia
Email: ichilan.itc@gmail.com, *Zgg64@163.com, adrianlab@foxmail.com, vinhteang.kaing@gmail.com, sokty@itc.edu.kh

How to cite this paper: Ich, I., Zhang, G.G., Li, A.B., Kaing, V. and Sok, T. (2023) Numerical Study on Hydraulic Characteristics and Discharge Capacity of Modified Piano Key Weir with Various Inlet/Outlet Width Ratio. *World Journal of Engineering and Technology*, **11**, 113-135.
https://doi.org/10.4236/wjet.2023.111009

Received: January 4, 2023
Accepted: February 25, 2023
Published: February 28, 2023

Abstract

A modified piano key weir with a rounded nose and a parapet wall (MPKW) can improve the discharge capacity significantly compared to a standard piano key weir. However, the optimum of the inlet/outlet width ratio (Wi/Wo) on the discharge efficiency of MPKW is still not investigated numerically. The present work utilized the numerical modeling to investigate and analyze the effects of the inlet/outlet key width ratios on the hydraulic characteristics and discharge capacity of the MPKW. To validate the numerical model with the experimental data, the results indicate that the average relative error is 2.96%, which confirms that the numerical model is fairly well to predict the specifications of flow over on the MPKW. Numerical simulation results indicated that the discharge capacity of the MPKW can be improved up to 8.5% by optimizing the Wi/Wo ratio ranging from 1.53 to 1.67 even if the other parameters of the MPKW keep unchanged. A big Wi/Wo ratio generally leads to an increase in discharge capacity at low heads and a little effect on the discharge efficiency at high heads. The discharge efficiency of the inlet and outlet crests increases up to 9.6% for high heads, while discharge efficiency of the lateral crest decreases up to 23.5% compared with the reference model. The findings of the study revealed that the intrinsic influencing mechanism of the Wi/Wo ratio on the discharge performance of MPKWs.

Keywords

Discharge Capacity, FLOW-3D, Hydraulic Characteristics, Numerical

Simulation, Modified Piano Key Weir, Parameter Optimization

1. Introduction

A piano key weir (PKW) is a nonlinear and labyrinth-type spillway weir, which was first introduced by Hydrocoop in France [1] and proposed by Lempérière and Ouamane [2]. The innovative design of the labyrinth weir replaces the traditional vertical design with an upstream/downstream overhang extension, extending the spillway crest and reducing the basement of the weir. According to Anderson and Tullis [3], the PKW is approximately 20% more efficient than the traditional labyrinth weir, and it solves most problems compared with the original labyrinth weir, such as 1) its small footprint makes the PKW an efficient, 2) it may be easily installed even at very limited foundation space, 3) its ability to pass large flows without the operation and maintenance issues, and 4) cost-effective solution for the increase of the flood releasing capacity at existing concrete gravity dams. Moreover, the PKW proved to be a cost-effective solution both for rehabilitation and for new dam projects with a high level of limitations (e.g., limited space, high specific flood discharge, small reservoir level variation, etc.) compared with the design discharge to be released [2]. Ribeiro, *et al.* [4] reported that the structure of a PKW is more complex than a labyrinth weir, for a PKW has additional geometric parameters, and the choice of each parameter significantly impacts discharge. Due to the large number of geometrical parameters for this type of structure, a naming convention was proposed by Pralong, *et al.* [5] to unify the definitions and notations (see **Figure 1(a)**). The PKW's geometric parameters have been widely researched due to their successful application in hydraulic engineering. There have been more than 35 PKWs under construction or already constructed around the world in the past 15 years, and research continues to develop the knowledge throughout the globe [6].

Several experimental studies and three-dimensional (3D) computational fluid dynamics (CFD) simulations on PKWs with different geometries have been conducted to develop a better understanding of flow behavior and to identify the primary and secondary parameters influencing its discharge capacity and hydraulic performance [7]-[14]. The magnification ratio (L/W) and weir height (P) was reportedly the primary parameters that dominate the discharge capacity of a PKW, whereas overhang ratio (Bi/Bo) and key width ratio (Wi/Wo) were identified as secondary parameters [12] [13] [15] [16] [17]. Lempérière [18] reported that the discharge capacity of the PKW and its construction cost are optimally balanced when L/W = 5. Lempérière, *et al.* [19] reported that PKW models with Bo/Bi > 1 have higher discharge efficiency than those with Bo/Bi < 1. Machiels, *et al.* [20] determined the major geometric parameters that affect discharge capacity when L/W is fixed, namely, the height P, the upstream/downstream overhang ratio Bi/Bo and the inlet/outlet width ratio Wi/Wo. Through a combina-

tion of numerical simulation and model tests, Li, *et al.* [21] demonstrated the influence of the height P on the discharge capacity of a PKW, and some scholars conducted many researches on the other geometric parameters either, such as the form of the noses [22], the wall thickness [23], and the geometric shape of the alveoli [24], providing substantial contributions to the design and application of PKWs.

As one of the critical parameters of a PKW, the Wi/Wo ratio has been studied by numerous research scholars [10] [12] [15] [16] [26]. Ouamane and Lempérière [15] investigated three types of PKW (Wi/Wo = 0.67, 1.0, and 1.5), and the results indicated that the discharge capacity increases with the increasing Wi/Wo. Lempérière [18] suggested that the optimal value of Wi/Wo is 1.25. Based on abundant test data, Ribeiro, *et al.* [4] suggested that a ratio of Wi/Wo = 1.6 is a good compromise. Anderson and Tullis [3] and [26] investigated the discharge capacities of eight types of PKW and suggested that the PKW has the highest discharge efficiency when Wi/Wo falls between 1.25 and 1.5. However, an additional investigation was not performed for scenarios where Wi/Wo exceeded 1.5. Machiels, *et al.* [12] demonstrated that Wi/Wo ratios between 1.29 and 1.57 provide the optimal discharge capacity of the weir height. Moreover, Li, *et al.* [10] investigated Wi/Wo ratio numerically and thought that the discharge capacity of PKW increases with the increasing Wi/Wo when Wi/Wo > 1, especially for low water levels. Generally, most previous studies focused on the experimental and numerical influence of Wi/Wo on the discharge efficiency of standard PKWs. However, none of them recommended the optimum Wi/Wo ratio on the discharge efficiency of the modified piano key weir with a rounded nose and a parapet wall (see **Figure 1(b)**). Moreover, it remains unclear how the Wi/Wo ratio affects the hydraulic performance of MPKWs and whether there is an optimal ratio.

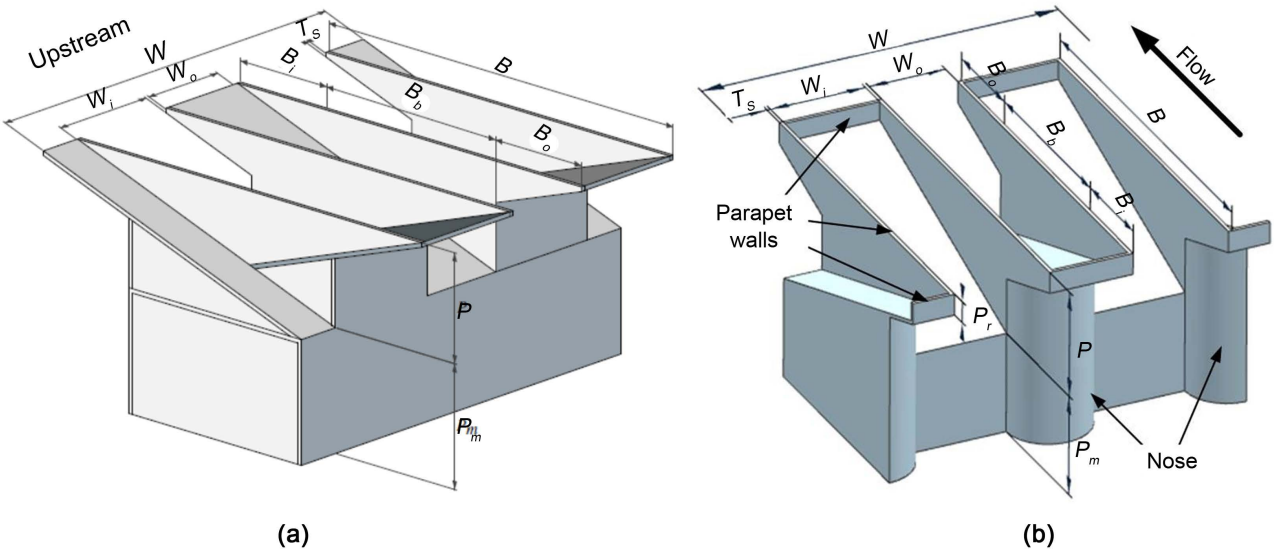

Figure 1. Three-dimensional view of (a) a standard type-A PKW and (b) a modified piano key weir (MPKW) adapted from Li [25] and Li, *et al.* [11].

In the present study, FLOW-3D® was used to simulate the hydraulic characteristics and discharge capacity of nine MPKWs with different inlet/outlet width (Wi/Wo) ratios in order to clarify the hydraulic characteristics (e.g., flow fields, free surface elevations and flow velocities) of the MPKWs and the effect of the Wi/Wo ratio on the discharge capacity of MPKWs under different upstream head conditions. Furthermore, the discharge capacity and efficiency of the inlet crest, outlet crest and lateral crest was investigated. Finally, an optimal range for the Wi/Wo ratio is proposed to provide a reference for the geometric design and engineering application of MPKWs.

2. Materials and Methods

2.1. Li's Experimental Description

In order to confirm the performance and predictability of the present numerical study, experimental data by Li [25] and Li, *et al.* [11] were used. In Li [25]'s experiments, a horizontal rectangular flume facility with a length, width, and depth of 16 m, 0.5 m, and 0.75 m, respectively, was used (see **Figure 2**). The flume system is equipped with an automatic flow-regulating device and automatically detects variations in the discharge and upstream flow depth data, which were obtained with an electromagnetic flow meter and a water level gauge with accuracies of 1% full span and ±0.1 mm, respectively. To facilitate flow visualization, the bed and lateral crests of the test channel were fabricated with tempered glass. The flume facility intake was equipped with a 1-m-thick perforated plastic sheet to ensure uniform flow conditions. The main equipment used during the test included the flume body, water supply, and return system, automatic

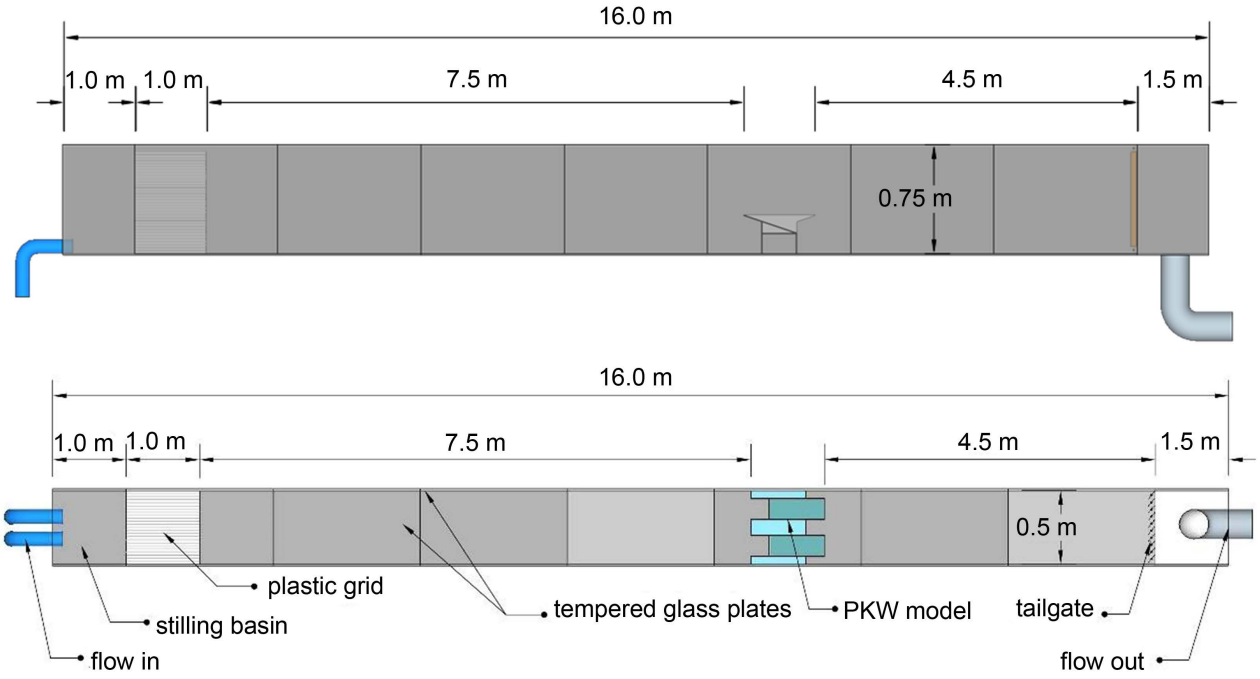

Figure 2. Schematic of the flume facility used for the experimental adapted from Li [25].

flow-acquisition equipment, and tailgate automatic control system (more details see Li [25] and Li, *et al.* [11]).

2.2. Input Parameters for Numerical Models

The detailed geometric characteristics of the modified piano key weir model (abbreviated as MPKW) and the layout of the model are presented in **Table 1** and **Figure 3**, respectively.

2.3. Numerical Model

2.3.1. Governing Equation and Turbulence Model

The Renormalization Group (RNG) *k-ε* turbulence model has been successfully applied in many numerical simulations of labyrinth weirs and piano key weirs by numerous researchers, with good accuracy based on the results of the numerical investigation, such as Sangsefidi, *et al.* [27], Safarzadeh and Noroozi [28], Crookston, *et al.* [8], Chahartaghi, *et al.* [29], Ghanbari and Heidarnejad [30] and Li, *et al.* [31]. Moreover, a small number of encrypted grids and high calculation efficiency are required on the wall. So the Renormalization Group (RNG) *k-ε* turbulence model was used in this study to investigate the hydraulic characteristics and discharge capacity of MPKWs, as also recommended by FLOW-3D [32]. The RNG *k-ε* governing equations are as follows:

Continuity equation:

Table 1. Geometric characteristics of the numerical and physical model of the MPKW (mm) by Li [25].

Baseline Model	P_m	P	W_i	W_o	W	$B_i = B_o$	B	T_s
Numerical and Physical	141.7	125	133.3	106.7	500	125	500	5

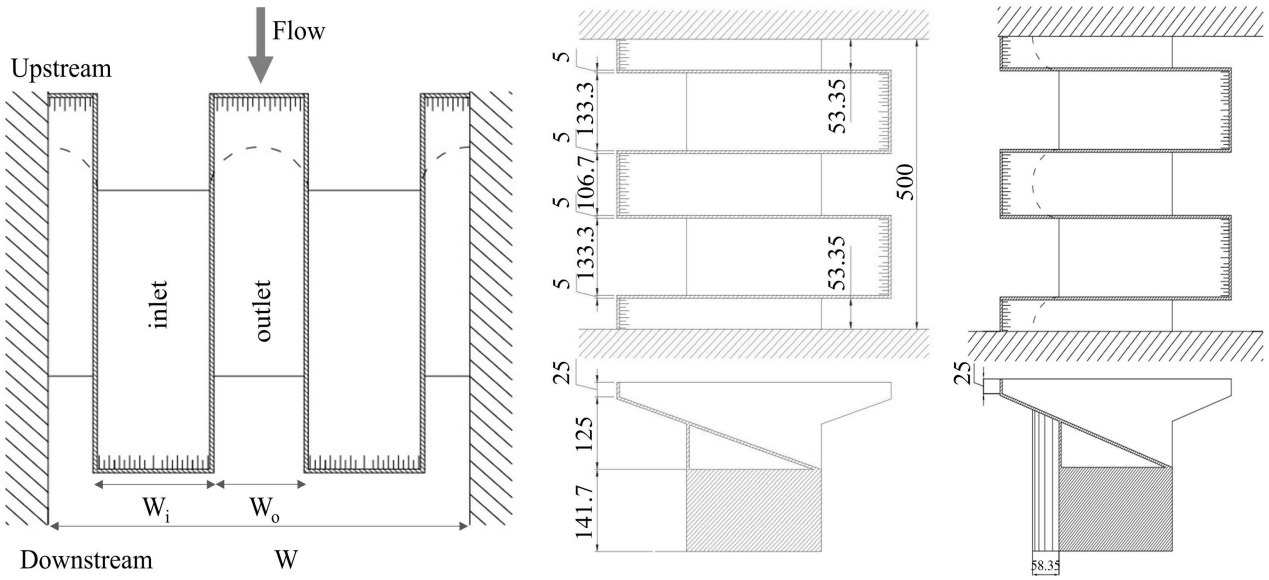

Figure 3. Schematic of the flume facility used for the experimental adapted from Li [25].

$$\frac{\partial \rho}{\partial t}+\rho\frac{\partial u_i}{\partial x_i}=0 \tag{1}$$

RANS equation:

$$\frac{\partial \rho\overline{u_i}}{\partial t}+u_i\frac{\partial \rho\overline{u_iu_j}}{\partial x_i}=\mu\frac{\partial}{\partial x_j}\left(\frac{\partial \overline{u_i}}{\partial x_j}\right)-\frac{\partial \overline{p}}{\partial x_i}+\frac{\partial\left(-\rho\overline{u_i'u_j'}\right)}{\partial x_j} \tag{2}$$

k equation:

$$\frac{\partial \rho k}{\partial t}+\frac{\partial \rho k u_i}{\partial x_i}=\frac{\partial}{\partial x_j}\left(\alpha_k\mu_{eff}\frac{\partial k}{\partial x_j}\right)+G_k+\rho\varepsilon \tag{3}$$

ε equation:

$$\frac{\partial \rho\varepsilon}{\partial t}+\frac{\partial \rho\varepsilon u_i}{\partial x_i}=\frac{\partial}{\partial x_j}\left(\alpha_\varepsilon\mu_{eff}\frac{\partial \varepsilon}{\partial x_j}\right)+\frac{C_{1\varepsilon}^*\varepsilon}{k}G_k-C_{2\varepsilon}\rho\frac{\varepsilon^2}{k} \tag{4}$$

In Equations (1)-(4), k is the turbulent kinetic energy, ε is the turbulent dissipation rate, ρ is the fluid density, u is the velocity, p is the pressure, t is the time, μ is the dynamic viscosity of the fluid, $-\rho\overline{u_i'u_j'}$ is the Reynold's stress, μ_{eff} is a diffusion coefficient ($\mu_{eff}=\mu+\mu_t$, μ_t being the eddy viscosity), α_k and α_ε are the model constants ($\alpha_k=\alpha_\varepsilon=1.39$), G_k is the turbulent kinetic energy generation term, and $C_{2\varepsilon}$ is a model constant ($C_{2\varepsilon}=1.68$). $C_{1\varepsilon}^*=C_{1\varepsilon}-\frac{\eta(1-\eta/\eta_0)}{1+\beta\eta^3}$, including the constants $C_{1\varepsilon}=1.42$, $\eta_0=4.377$, $\beta=0.012$, $\eta=\left(2E_{ij}\cdot E_{ij}\right)^{\frac{1}{2}}\frac{k}{\varepsilon}$, $E_{ij}=\frac{1}{2}\left(\frac{\partial u_i}{\partial x_j}+\frac{\partial u_j}{\partial x_i}\right)$ is the time average strain rate, and $\mu_t=\frac{\rho C_\mu k^2}{\varepsilon}$ is the eddy viscosity coefficient, in which $C_\mu=0.0845$.

The volume-of-fluid (VOF) method was used to simulate the flow fields over MPKW [33]. The VOF transport equation solution was expressed by FLOW-3D [32], Safarzadeh and Noroozi [28], Abbasi, *et al.* [34] and Ghaderi, *et al.* [35] in Equation (5):

$$\frac{\partial F}{\partial t}+\frac{1}{V_F}\left[\frac{\partial\left(FA_xu\right)}{\partial x}+\frac{\partial\left(FA_yv\right)}{\partial y}+\frac{\partial\left(FA_zw\right)}{\partial z}\right]=0 \tag{5}$$

In the above equation, A is an average ratio of flow area along with (x,y,z) directions; (u,v,w) are the average velocities along with (x,y,z) directions, and F is the fluid ratio function, whose value is between 0 and 1. If $F=0$, the cell is completely full of air, and if $F=1$, the cell is completely full of water. Usually, a position with $F=0.5$ is defined thefree water surface.

2.3.2. Numerical Model Set-Up and Boundary Conditions

First, the MPKW numerical model was established, which has the same size as the experimental model by the Xi'an University of Technology [11] [25]. The values of the geometrical parameters of the model are demonstrated in **Table 1**. The inlet boundary was set to pressure inlet condition; the downstream outlet

condition was set to outflow; the inner boundaries were defined as symmetry. The top boundary was set as a pressure of o (atmospheric). No-slip wall boundaries were set along the whole surface of the MPKW model. The computational domain of the existing study and the boundary conditions are displayed in Figure 4.

2.3.3. Grid Convergence Analysis

A grid convergence index (GCI) is the most common and reliable technique for quantifying discretization uncertainty in numerical results, and determines the computed free surface profiles of the three grids [36]. To investigate the influence of the mesh resolution, the GCI method was used to estimate the accuracy of the numerical results with three different meshes with fine, medium, and coarse cells, corresponding to the total cell numbers of 5,766,904 and 2,978,296 and 1,758,264, respectively. Details of the three computational grids are summarized in Table 2.

The fine-grid convergence index is defined the Richardson error estimator as follows,

$$GCI_{32}^{fine} = \frac{1.25|E_{32}|}{r_{32}^{p}-1} \tag{6}$$

where, $E_{32} = (\phi_{s2} - \phi_{s3})/\phi_{s2}$ is the approximate relative error between the medium and fine grids; ϕ_{s2} and ϕ_{s3} are the discharge solutions for the medium

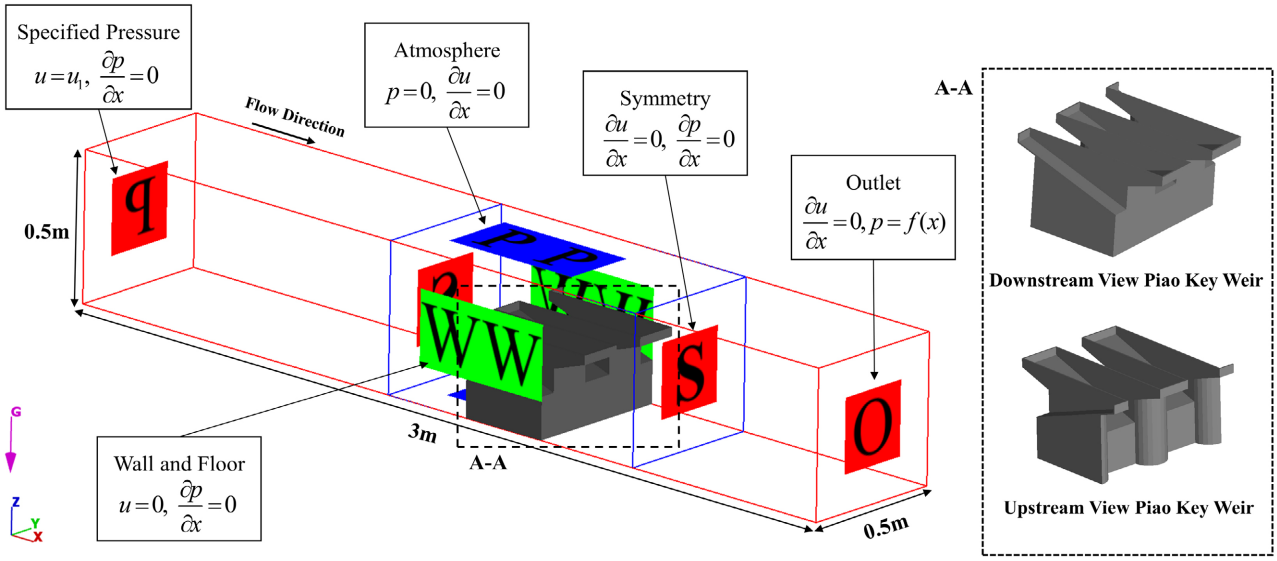

Figure 4. Applied boundary conditions on a numerical domain in FLOW-3D®.

Table 2. Characteristics of the computational grids.

Mesh	Containing Block Cell Size (mm)	Nested Block Cell Size (mm)	Computing time (h)
1	4	8	73.8
2	5	10	25.5
3	6	12	14.5

and fine grid, respectively; and p denotes the local order of accuracy [34] [36]. The values of p for the three-grid solutions are obtained by solving the following equation:

$$p = \frac{1}{\ln r_{32}} \ln \frac{\left(r_{32}^{p} - 1\right) e_{21}}{\left(r_{21}^{p} - 1\right) e_{32}} \tag{7}$$

where, $e_{21} = \phi_{s2} - \phi_{s1}$, $e_{32} = \phi_{s3} - \phi_{s2}$ and $r_{21}^{p} = G_2 / G_1$ are the grid refinement factor between the fine and medium grids, and $r_{32}^{p} = G_3 / G_2$ is referred to as the grid refinement factor between the medium and coarse grids (for the existing three-grid comparisons $G_1 < G_2 < G_3$) [34] [36].

Table 3 illustrates the GCI estimations and the relative change between two adjacent meshes. GCI_{21} and GCI_{32} are the relative changes both from medium to coarse and from fine to medium mesh, respectively. From these obtained results, it is found the value of $GCI_{32} / r^{p} GCI_{21}$ close to 1, indicating that the solution is within the approach range of convergence. Consequently, a grid mesh with 2,978,296 cells, as well as a containing block with a cell size of 10 mm and a nested block of 5 mm was selected (Figure 5). To reduce the effect of

Table 3. The numerical results of mesh convergence analysis.

Parameters	Amounts
ϕ_{s1} (−)	30.01
ϕ_{s2} (−)	31.14
ϕ_{s3} (−)	35.85
p (−)	6.37
E_{32} (%)	3.78
E_{21} (%)	15.11
GCI_{21} (%)	1.50
GCI_{32} (%)	8.60
$GCI_{32} / r^{p} GCI_{21}$	0.97

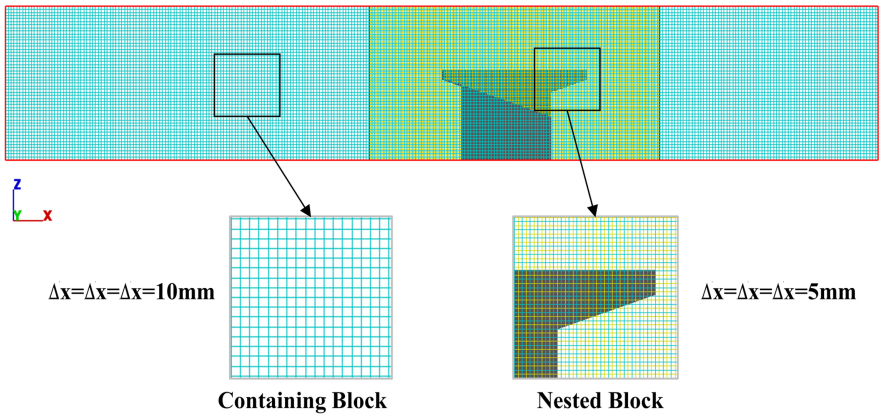

Figure 5. A typical 3D view (top) and side view (bottom) of the numerical mesh setup.

computational mesh on simulation results, the same mesh was applied to all models of this research. Computations in the viscous sub-layer were prevented. The first node was located near a wall in order to keep the dimensionless parameter of y^+ (Equation (8)) in the range of $5 < y^+ < 30$ [37].

In this study, it spent 14.5 to 73.8 h to simulate the different cases for a workstation computer with 12 cores (Intel® Xeon® Silver 4116 CPU @ 2.10 GHz and 64 GB RAM). Also, for controlling the satisfaction of the continuity equation, the time series of the inlet discharge is compared to the outflow discharge from the upstream boundary and downstream of the weir. Analyses showed that a 10-second period is sufficient for model convergence (**Figure 6**).

2.3.4. Numerical Cases

In this study, 90 simulation cases were performed by FLOW-3D for nine MPKWs with various Wi/Wo ratios (Wi/Wo = 0.5, 0.66, 0.8, 1, 1.25, 1.53, 1.67, 1.82 and 2). The other geometry size is the same such as the vertical weir height P, transverse width W, streamwise length B and the total length of the MPKW's spillway front L (*i.e.*, the sum of the inlet width and the outlet width) are fixed as well. During the simulations, H and the corresponding relative water head H/P condition for each Wi/Wo vary between 15 mm and 131 mm and between 0.12 and 1.05, respectively. Details of the model dimensions are listed in **Table 4**.

3. Model Verification

The numerical results were validated by Li'sexperimental data [25]. In the test geometry, Wi/Wo is 1.25 in the verification phase, and the other model dimensions are consistent with the numerical simulation model (**Table 1**). After the numerical simulation of steady-state flow over the MPKW had been completed, a comparison was performed between numerical and experimental results to validate the model. The error between data obtained from FLOW-3D® and experimental data was made by using mean absolute relative error (MARE) according to Equation (8):

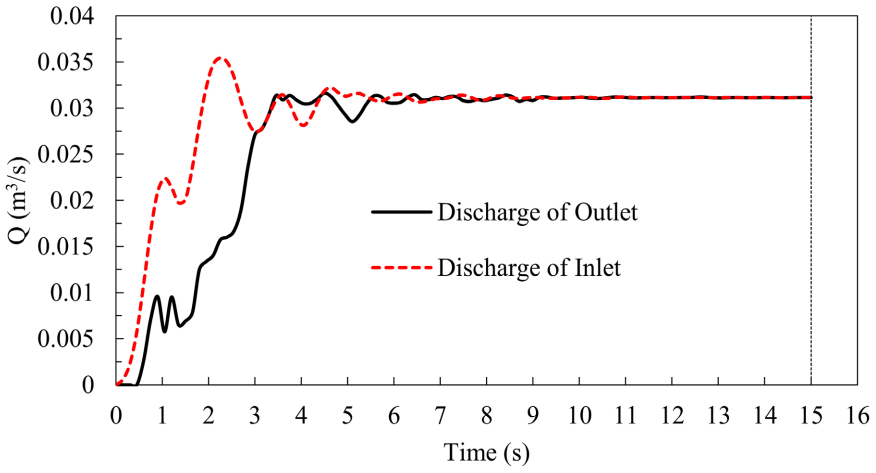

Figure 6. Solution convergence for inflow and outflow discharges for H/P = 0.32.

Table 4. Dimensions of the MPKWs with various W_i/W_o values.

Case number	W_i (mm)	W_o (mm)	W_i/W_o
1	80	160	0.50
2	95	145	0.66
3	106.7	133.3	0.80
4	120	120	1.00
5	133.3	106.7	1.25
6	145	95	1.53
7	150	90	1.67
8	155	85	1.82
9	160	80	2.00

$$\text{MARE} = \frac{1}{N}\sum_{i=1}^{N}\left|\frac{(O_i - P_i)}{O_i}\right| \times 100 \tag{8}$$

Here O_i is the measured discharge values, P_i is the simulated discharge values, and N is the total number of data. Figure 7 and Table 5 show discharge values and errors. It was found that there was a good agreement between the numerical and experimental results. The maximum relative error was 5.75% for H/P = 1.164, and the minimum relative error was 0.70% for H/P = 0.519 with a mean average relative error of 2.96%, which confirms the numerical model can be used to predict flow specifications over MPKWs accurately.

Figure 8 shows the flow pattern over the MPKW by numerical simulation at the low and high relative head, respectively. The outlet channels are not completely filled by water flow at the low head (H/P = 0.12), whereas the water surface is practically flat (**Figure 8(a)**). When the head increases (**Figure 8(b)**), the lateral overflow crests of the weir are gradually submerged. Moreover, the outlet channels are close to full capacity, a nappe collision occurs in the middle of the outlet keys, and a standing wave region occurs downstream of the outlet keys, whereas the water surface produces considerable decreases over the MPKW, corresponding to the experiment study by Li, *et al.* [11]. Therefore, with the increase of the water head, the discharge capacity of the MPKW gradually decreases, obtained by the numerical simulation is consistent with the experimental results [11].

4. Results

4.1. Discharge Capacity

4.1.1. Total Discharge Capacity and Discharge Efficiency

In order to assess the discharge efficiency, the concept of the discharge amplification ratio "r" that used the ratio of the discharge of the piano key weir to that of the linear sharp-crested weir under the same conditions is proposed by Ribeiro, *et al.* [16], was applied to assess the efficiency, discharge capacity of the

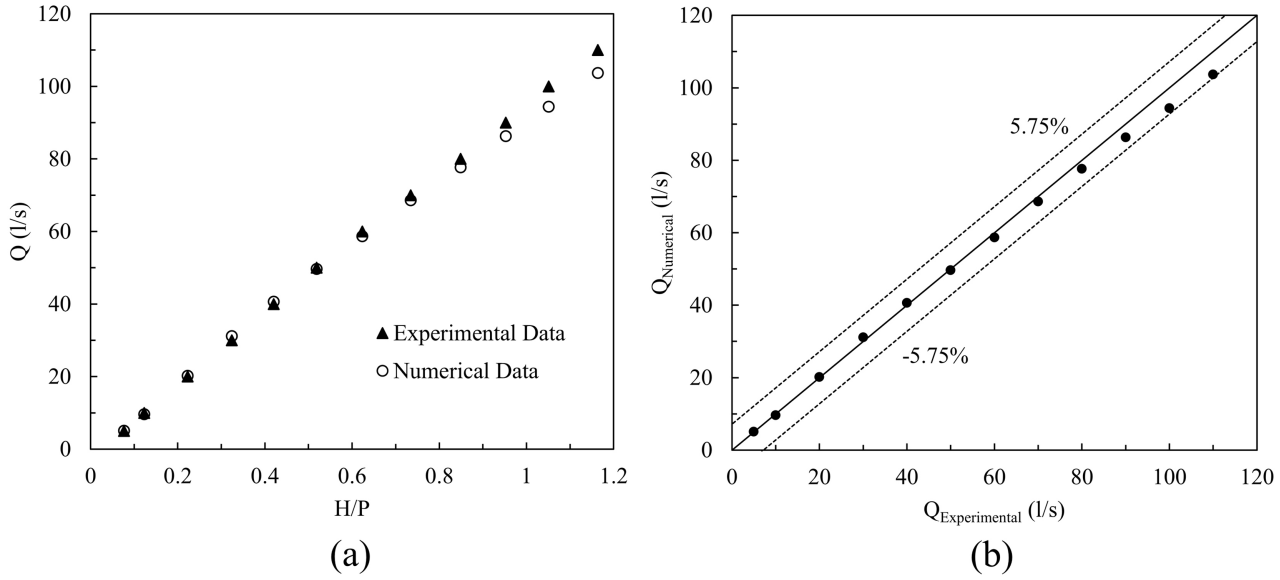

Figure 7. (a) Comparison of discharge values obtained from numerical solution with experimental data; (b) Determination of error percentage.

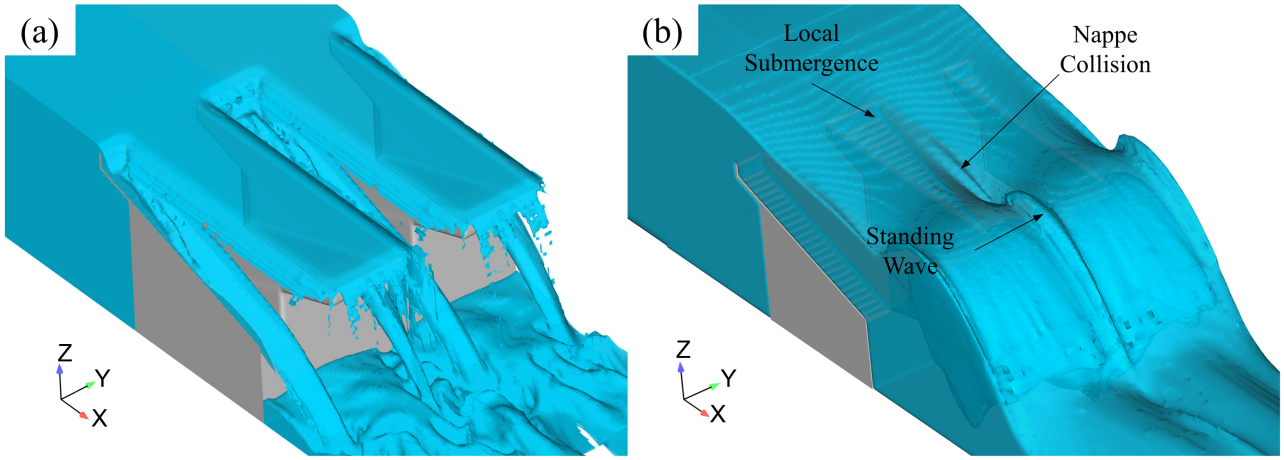

Figure 8. A typical 3D flow field obtained at different relative head condition of (a) low (H/P = 0.12) and (b) high (H/P = 1.05).

piano key weir as given in Equation (9):

$$r = \frac{Q_{pkw}}{Q_{scw}} \tag{9}$$

In the present study, the basic formula for the discharge capacity Q_{scw} of the traditional linear sharp-crested weir attends as a reference was developed by Gharahjeh, *et al.* [38], which is given as follows:

$$Q_{scw} = C_{scw} L \sqrt{2g} H^{3/2} \tag{10}$$

where $C_{scw} = 0.42$ is the discharge coefficient [39] [40], and L is the total width of the sharp-crested weir.

The general discharge formula of a PKW can be determined using the equation of the traditional linear sharp-crested weir, which represents all factors

Table 5. MAREvalues for the discharge values versus different H/P ratios on PKW.

Case number	H (mm)	H/P	Q-Measured values (l/s)	Q-Simulated values (l/s)	MARE (%)
1	9.6	0.08	5	5.0904	1.81
2	15.4	0.12	10	9.5968	4.03
3	27.8	0.22	20	20.1855	0.93
4	40.5	0.32	30	31.1427	3.81
5	52.5	0.42	40	40.6618	1.65
6	64.9	0.52	50	49.6515	0.70
7	78.0	0.62	60	58.7062	2.16
8	91.8	0.73	70	68.5836	2.02
9	106.2	0.85	80	77.6699	2.91
10	119.1	0.95	90	86.3103	4.10
11	131.4	1.05	100	94.4000	5.60
12	145.5	1.16	110	103.676	5.75
			Mean		2.96

affecting the discharge capacity of the PKW as a discharge coefficient C_{dw} [15]:

$$Q_{pkw} = C_{dw} W \sqrt{2g} H^{3/2} \tag{11}$$

Here C_{dw} is a dimensionless coefficient, and its value is not fixed; Q_{pkw} is a discharge over the weir; g is the acceleration of gravity; W is the total width of the weir, and H is the upstream water head. The empirical formulas for C_{dw} have been proposed by Ribeiro, *et al.* [16], Kabiri-Samani and Javaheri [17], Machiels [41] and Li, *et al.* [11] in recent years.

To detect the effect of Wi/Wo on discharge efficiency and capacity, nine MPKW models, described herein as Wi/Wo = 0.5 to 2, were prepared. The results show that the discharge efficiency is highly influenced by the change in Wi/Wo ratio, as shown in **Figure 9**, where the Wi/Wo > 1.25 is hydraulically performing better than other Wi/Wo ratios where the discharge amplification ratio value is higher than the values of discharge amplification ratio of other Wi/Wo ratios for a given discharge when the relative head is extremely low. Moreover, a larger Wi/Wo = 2 produces a more hydraulically efficient discharge up to 6 times as efficient as a linear sharp-crested weir. For H/P = 0.22, the discharge efficiency with Wi/Wo values of 2 and 1.67 is around 5 times higher than the linear sharp-crested weir. However, as the relative head continues to rise, the MPKW with a larger Wi/Wo becomes less effective. For example, when H/P > 0.32, the discharge efficiency with a Wi/Wo = 2 is less than that of the model with Wi/Wo value of 1.25. Generally, although the MPKW discharge increases with the increasing relative head, the amplification efficiency rapidly decreases as the relative head rises. When H/P > 0.95, the amplification efficiency of the MPKWs with various Wi/Wo ratios is approximately 2 times higher than that of

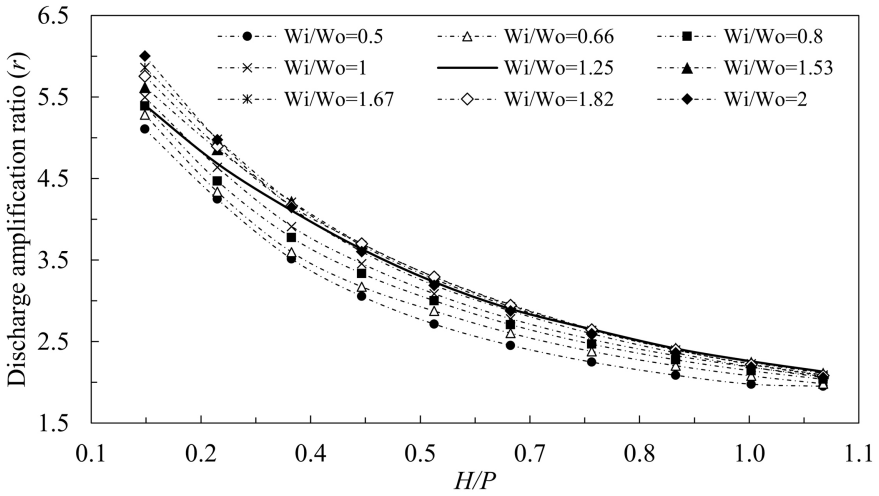

Figure 9. The relationship between discharge amplification ratio (r) with H/P under different Wi/Wo ratios.

the linear sharp-crested weir, and the discharge amplification efficiency becomes non-significant.

Using a MPKW with Wi/Wo = 1.25 as a reference model, the influence of varying Wi/Wo ratios was evaluated. **Figure 10** shows the relationship between the relative discharge capacity (Q_{Rel}) for all tested MPKWs and the relative water head H/P compared with the reference model. Thereby, Q_{Rel} was calculated via $Q_{Rel} = Q_{Ratio} - Q_{Wi/Wo=1.25} / Q_{Wi/Wo=1.25}$ based on numerical simulation data, where the subscript "Ratio" indicates the Wi/Wo ratio from the relevant model.

Results indicate that MPKW configurations with Wi/Wo > 1.25 generally show a better performance in terms of discharge capacities than those with Wi/Wo < 1.25, especially for low relative heads with H/P < 0.73. Compared to the reference model with Wi/Wo = 1.25, up to approximately an 11% increase of the discharge coefficient can be achieved for low relative heads by expanding the Wi/Wo ratio, even though the rounded nose and parapet wall and total crest length remain constant. For Wi/Wo > 1.25, almost of MPKWs show increases in discharge efficiency (except Wi/Wo = 2 and H/P > 0.62). For low heads (H/P ≤ 0.22), a large Wi/Wo produces a large increase in the discharge efficiency. However, the discharge efficiency decreases continuously with the increasing water head, and for H/P > 0.32, the efficiency remains smaller than that of the reference model. While non-significant differences are observed in the discharge efficiencies of MPKWs with Wi/Wo > 1.25 for H/P = 0.42 - 0.73, the highest discharge efficiency in these cases is achieved by the MPKWs with Wi/Wo ratios of 1.53 and 1.82. For H/P = 0.85, the efficiency remains similar to that of thereference model for the MPKWs with Wi/Wo ratios of 1.53 and 1.67. Yet, at H/P > 0.85, the discharge efficiency decreases continuously with the increasing water head coincide. Wi/Wo ratios lower than 1.25 decrease the weir discharge capacity by up to 16% compared to the reference model. This suggests that the Wi/Wo range from 1.53 to 1.67 is close to the optimum ratio. Additionally, it can be

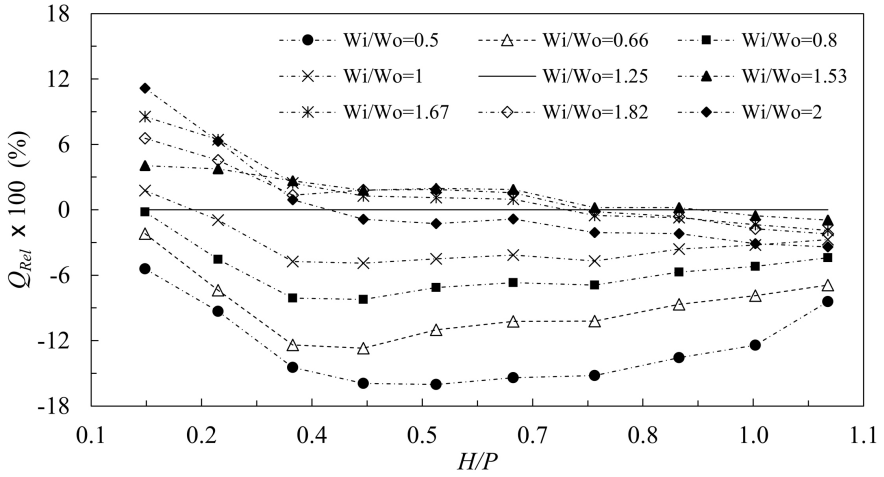

Figure 10. Relative effect of Wi/Wo on the total discharge capacity.

concluded that the ratios of Wi/Wo less than 1 and greater than 1.67 should be avoided in the design of MPKWs.

4.1.2. Discharge Capacities of the Inlet, Lateral, and Outlet Crests

According to the results of numerical simulations, the percentage discharge proportions of the upstream outlet crest, downstream inlet crest, and lateral crest relative to the overall weir discharge were derived, as shown in **Figure 11**. As a result, the percentage discharge proportion of the upstream outlet crest and downstream inlet crest (**Figure 11(a)**) increases and decreases oppositely depending on growing Wi/Wo ratios. As shown in **Figure 11(b)**, the percentage discharge proportion of the lateral crest increases with the developing Wi/Wo ratio and then falls back when Wi/Wo reaches 1.67. In this particular geometric configuration of MPKW, Wi/Wo = 1.67 appears to be the critical ratio from which the adverse effect begins to impact the discharge capacity. For MPKW models with Wi/Wo < 1.67, the benefit from velocity reduction is dominant; therefore, the discharge capacity rises with growing Wi/Wo ratios (see also **Figure 11**).

The magnitudes of the discharge values for the inlet, lateral, and outlet crests in all conditions using the advantages of numerical simulation are obtained unconnectedly. Based on the previously mentioned concept, the discharge amplification ratio per unit width R is defined as $R = q_{Wi/Wo} / q_{Wi/Wo=1.25}$. Since the weir width W is constant, the sum of the inlet width and the outlet width is constant. Therefore, the relationship between the R-value of the sum of the inlet and outlet crests ($R_{inlet+outlet}$) and the lateral crest ($R_{lateral}$) and the relative water head H/P is plotted, as shown in **Figure 12**.

The inlet and outlet crests are presented in **Figure 12(a)**; when the relative head H/P ≤ 0.42, the relationship between the $R_{inlet+outlet}$ of each model and H/P is equivalent properly. For lower water heads, the $R_{inlet+outlet}$ values are almost the same for the MPKWs with different Wi/Wo ratios. When the relative water head H/P > 0.45, the $R_{inlet+outlet}$ values for Wi/Wo ratios less than 1.25 are somewhat

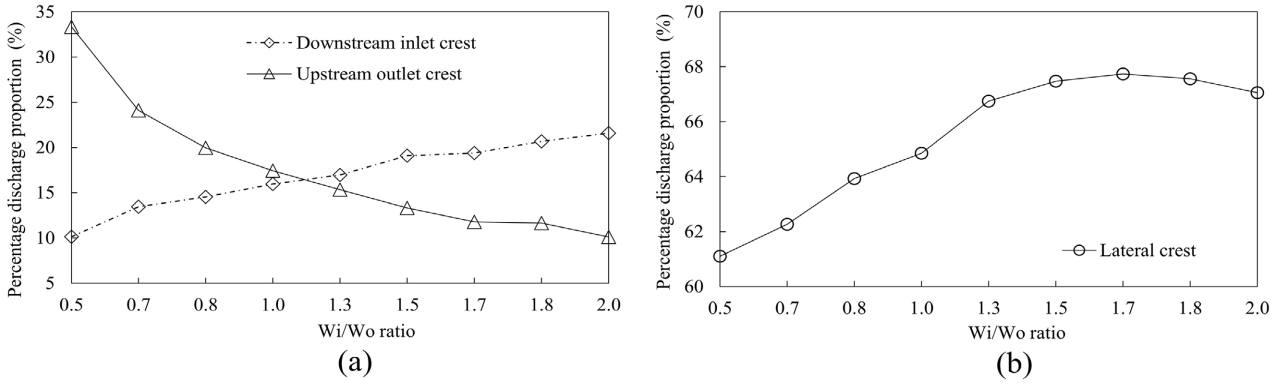

Figure 11. Percentage discharge proportion relative to total discharge at Q = 50 l/s (H/P = 0.52) for (a) upstream outlet crest and downstream inlet crest and (b) lateral crest.

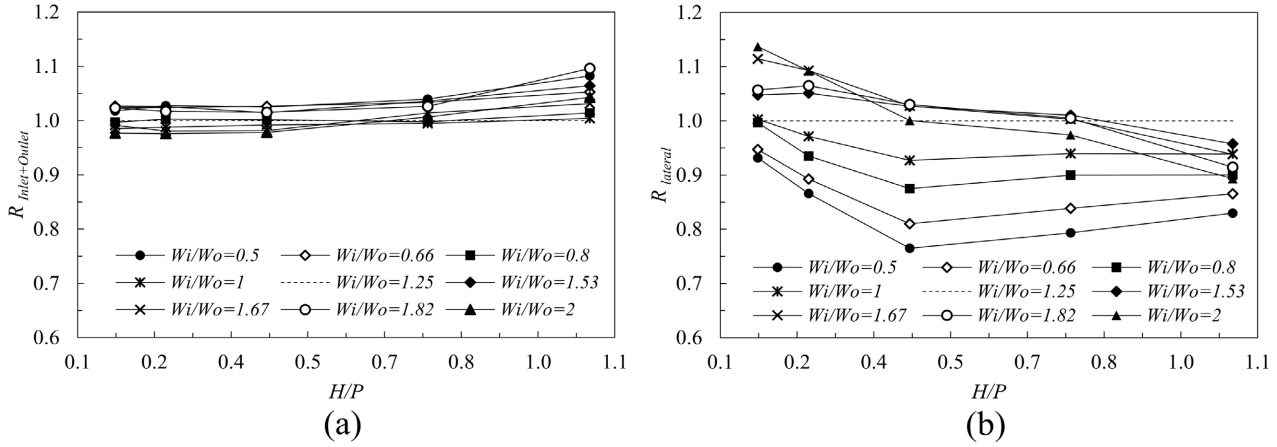

Figure 12. Relationship between R and H/P: (a) $R_{inlet+outlet}$ and (b) $R_{lateral}$.

smaller than that of the reference model. The $R_{inlet+outlet}$ values for Wi/Wo ratios greater than 1.25 exhibit an increase of 5% - 9% relative to the reference model with the rise in the Wi/Wo ratio. When the relative heads are lower, Wi/Wo ratios greater than 1.25 lead to increases in the discharge efficiency over the lateral crest. For H/P ≤ 0.26, the $R_{lateral}$ for a Wi/Wo ratio of 2 exhibits a maximum increase of 14% relative to that of the reference model (**Figure 12(b)**). As the relative head increases, the discharge efficiency over the lateral crest decreases, and the larger Wi/Wo is the faster the discharge efficiency declines. When H/P = 0.42, $R_{lateral}$ for a Wi/Wo ratio of 2 starts to fall behind $R_{lateral}$ for Wi/Wo, equal to 1.25. When the relative head H/P > 0.86, the $R_{lateral}$ ratios of all MPKWs with Wi/Wo ratios greater than 1.25 are lower (a Wi/Wo of 2 exhibits a decrease of approximately 9.6%) than that of the reference model. Wi/Wo ratios lower than 1.25 decrease the efficiency of the lateral crest by up to 23.5% compared to the reference model.

4.2. Flow Field Structure Analysis

4.2.1. Efficiency Free Surface Elevation Analysis

The flow through the MPKW is divided into three parts: the inlet crest, the out-

let crest, and the lateral crest depending on whether low (H/P = 0.12), middle (H/P = 0.52), and high (H/P = 1.05) head conditions. The detailed observation of the free surface elevation and its features describe the effect of the Wi/Wo ratio on the MPKW discharge efficiency. The discharge mechanism of the lateral crest is analyzed using flow surface profiles along the flow direction of the central section of the inlet key (Z = 0.125 m) and the outlet key (Z = 0.25 m). A middle head condition H/P = 0.52 (**Figure 13**) and a high head condition H/P = 1.05 (**Figure 14**) are evaluated as typical operating conditions.

According to **Figure 13(a)**, when Wi/Wo is 0.5, the lowest flow surface elevation is obtained for a middle head condition, and a large vertical contraction occurs at the inlet key section. In the outlet key section (**Figure 13(b)**), the flow surface curves are below the weir crest in the central section of the weir and increase to above the weir crest for MPKWs with Wi/Wo ≤ 1.25. For a high head, as the inlet/outlet width ratio increases, the flow surface elevations also increase

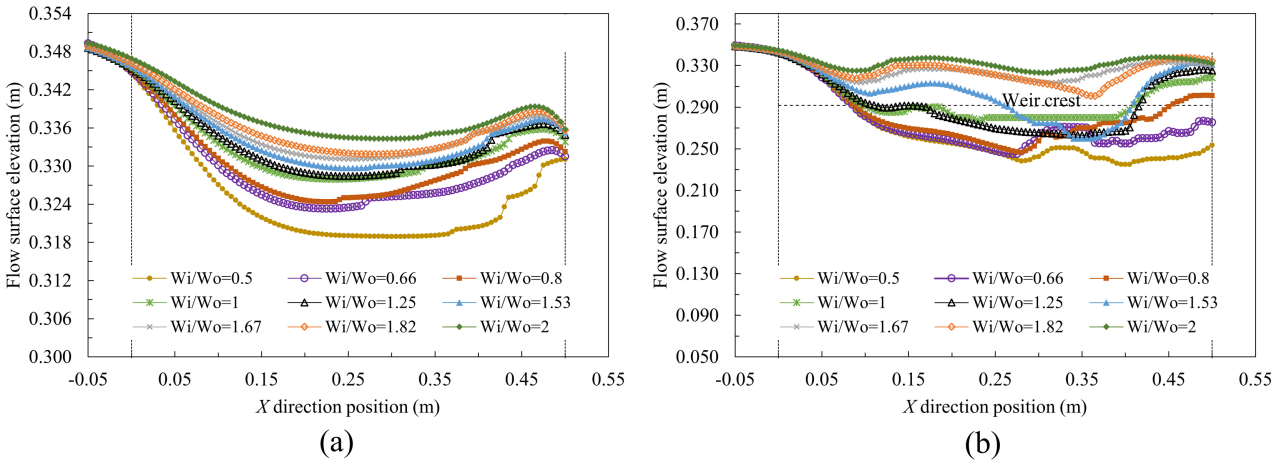

Figure 13. Flow surface curves for a middle head (H/P = 0.52): (a) the central section of the inlet key (Z = 0.125 m) and the central section of the outlet key (Z = 0.25 m).

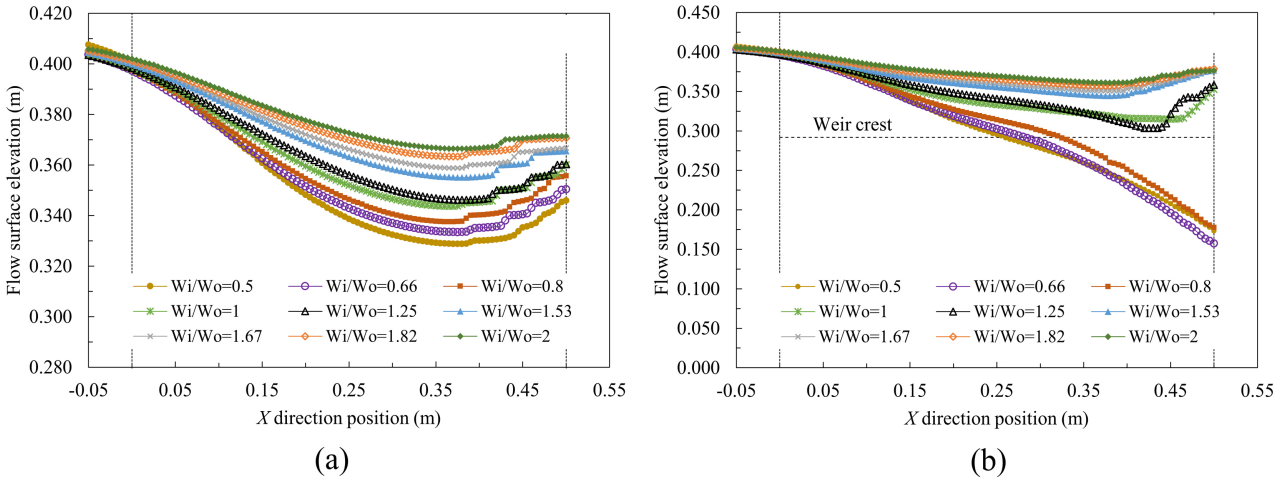

Figure 14. Flow surface curves for a high head (H/P = 1.05): (a) the central section of the inlet key (Z = 0.125 m) and the central section of the outlet key (Z = 0.25 m).

at the inlet key section (Figure 14(a)). However, the flow surface elevations in the outlet key section are above the weir crest for MPKWs with Wi/Wo ≥ 1 (Figure 14(b)). This finding indicates that the two streams of nappes that flow from the adjacent lateral crests to the outlet key are thick when head H/P is high and that the collision of the nappes causes an increase in the flow surface elevation.

Figure 15 compares the cross-sectional views of the PKW free surface profile with Wi/Wo ratios of 0.5, 0.8, 1.25, 1.67 and 2 when H/P = 0.52 (h = 64.9 mm). The position is located at X = 0.25 m (0.25 m downstream from the upstream apex of the PKW). For the PKW with a Wi/Wo of 0.5 (Figure 15(a)) and 0.8 (Figure 15(b)), the outlet key is wide enough, and the nappes from the lateral crests are relatively thin such that the nappes are not affected by the outlet width. The nappes neither collide in the outlet keys nor hinder the downstream discharge. Conversely, for the PKWs with Wi/Wo of 1.25 (Figure 15(c)) and 0.153 (Figure 15(d)), the nappes from both lateral crests collide with the nappe in the outlet key at an elevated location, hindering the flow toward the downstream channel. Similarly, Li, *et al.* [10] attest that the lateral flow regime is similar to the submerged discharge, and the spillway efficiency is significantly reduced.

4.2.2. Velocity Field Analysis

Figure 16 shows the velocity profiles in the inlet key centerline for H/P = 0.52 with Wi/Wo value ranging from 0.5 to 2 (extracted from numerical model results). Note a steady decrease in flow velocity with an increasing Wi/Wo ratio. Li, *et al.* [10] report that a lower flow velocity in inlet keys reduces the flow inertia in the longitudinal direction enabling a better flow approach and discharge distribution over the lateral crest, thus improving lateral crest efficiency. The same was found by Machiels, *et al.* [42] for lower heads, where the flow velocity

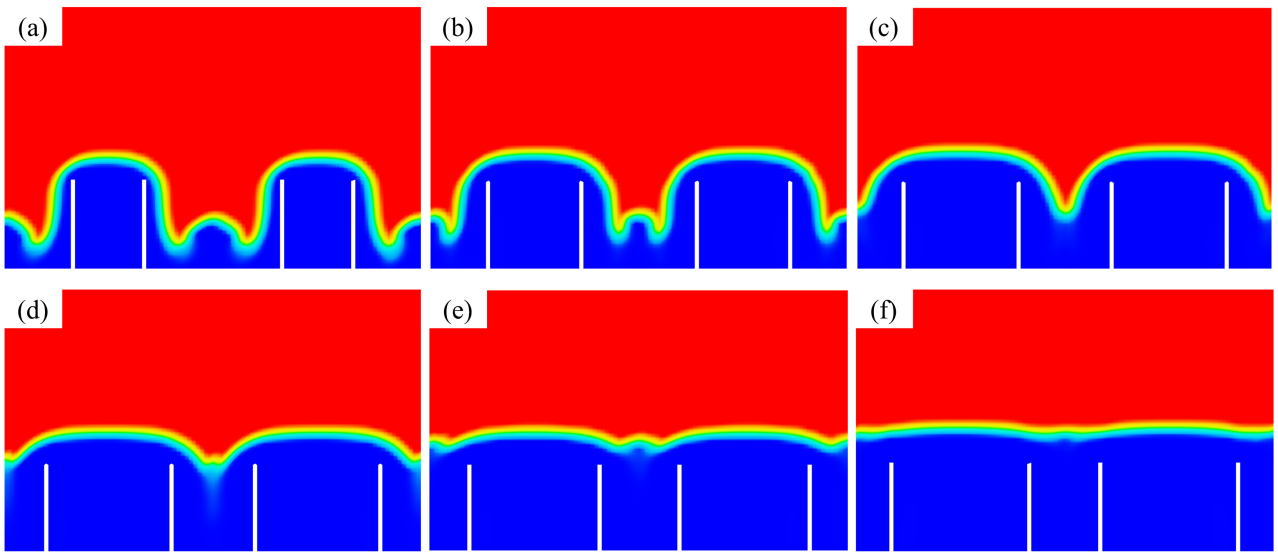

Figure 15. Cross-sectional views of fluid phases for middle head of H/P = 0.52: Wi/Wo = (a) 0.5; (b) 0.8; (c) 1.25; (d) 1.53; (b) 1.67; (b) 2.

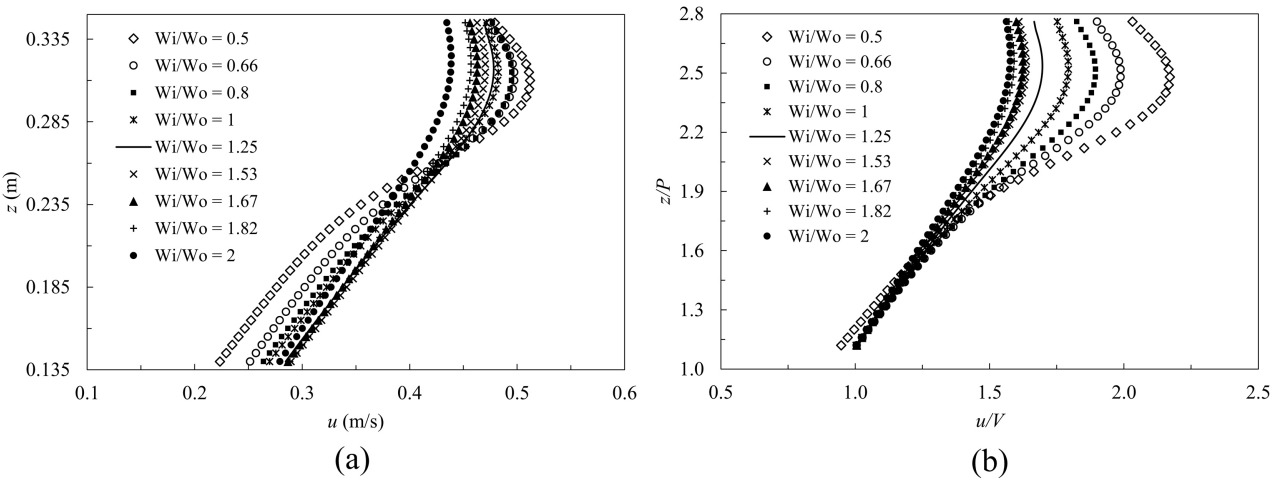

Figure 16. Exemplary velocity profiles in the inlet key centerline at different Wi/Wo ratios of the weir for H/P = 0.52: (a) dimensional value; (b) dimensionless value.

is largely responsible for the weir efficiency; a lower velocity increases the weir capacity. The Wi/Wo ratio can increase total weir efficiency by increasing the inlet cross-section and reducing the inlet key flow velocity.

5. Discussion

Generally, the auxiliary geometric parameters, such as the dam height, wall thickness, nose form, parapet walls, and crest shape, affect the discharge capacity of PKWs. The parapet wall was provided with a good opportunity for future PKW rehabilitations, enabling, in some cases, an increase in the discharge capacity by up to 20% according to Machiels, *et al.* [42], 15% according to Ribeiro, *et al.* [43], and 4.3% according to Anderson and Tullis [3]. Li, *et al.* [11] also conducted tests to study the effect of the parapet wall on the discharge capacity by increasing up to 15.5% higher than that of the PKW model without a parapet wall. This increase in discharge efficiency is related to the decreased local submergence (increased outlet key volume) and reduced inlet entrance energy loss (increased inflow area) caused by adding the parapet wall. Although installing a rounded shapes nose under the upstream apex overhangs of the PKW increased the discharge capacity by up to 7% according to Ouamane and Lempérière [15], 2.8% according to Anderson and Tullis [3], and 8.5% according to Li, *et al.* [11] for more efficient for low water heads than a standard PKW model.

As a previous study proposed by Li, *et al.* [11], the efficiency of the PKW designed with a rounded nose and a parapet wall (MPKW) enables an increase in the discharge efficiency by 16.8% compared to the standard PKW model. Consequently, the finding of this study confirmed that adding a rounded nose and a parapet wall weir can improve the upstream flow pattern, as well as the hydraulic efficiency of the PKW and that a higher weir height (P) allows the benefits of increasing Wi/Wo ratio to be more significant. In addition to reducing inlet energy losses and separation bubbles (backflow) that occur in the front of the inlet

key, Machiels, *et al.* [20] and Li, *et al.* [31] suggest that reducing the inlet key inlet flow velocity by adding noses to the PKW upstream apexes may improve PKW discharge capacity by modifying the nature of the critical section in the inlet key and improving the discharge efficiency of the lateral PKW walls.

As a result of this study, when H/P is in the range of 0.12 - 1.05, the discharge capacity decreases rapidly. To explain this phenomenon, the velocity as flow streamlines under different water head conditions is presented (**Figure 17**). When the water head is relatively low, the flow direction of the inlet key separates to both sides over the lateral keys and flows to the outlet key (**Figure 17(a)**). Although with the increase of water heads (**Figure 17(b)** and **Figure 17(c)**), the flow direction of the inlet key flow to the outlet key decreases and flows straightly downstream. In this study, it can be observed that the separation bubbles do not occur in the front of the inlet key compared to the previous study by Li, *et al.* [31]. The finding of this study confirmed that installing parapet walls and noses beneath the upstream apex overhangs of the PKW produced a hydraulically more efficient inlet (reduced flow contraction, reduced energy loss, reduced separation bubbles, and their transverse width, and potentially modified critical flow section location) and increased discharge efficiency.

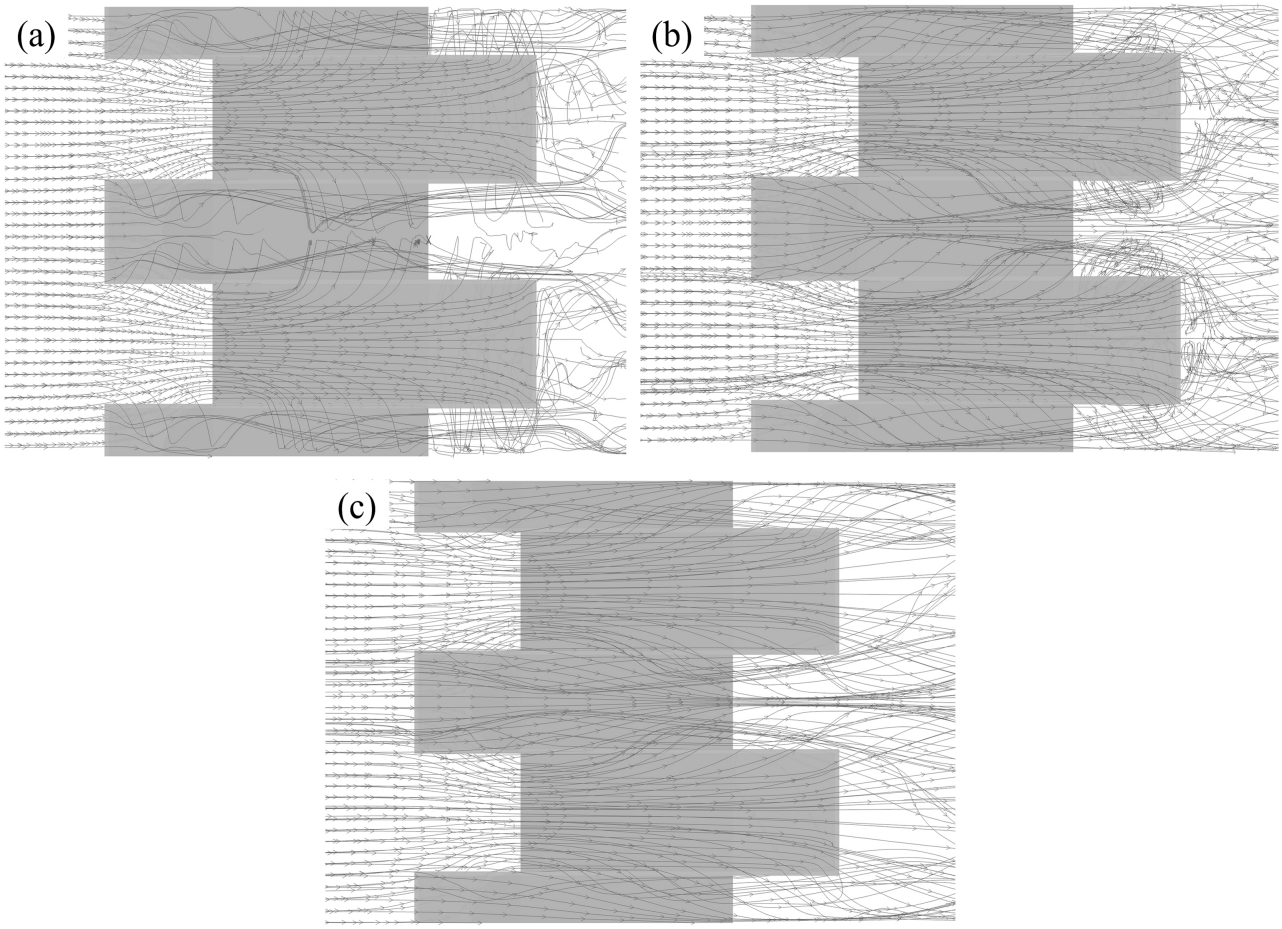

Figure 17. Flow streamlines with (a) low head (H/P = 0.12); (b) middle head (H/P = 0.52); (c) high head (H/P = 1.05).

6. Conclusions

The present study investigated the hydraulic characteristics and the discharge capacity of the modified piano key weir with varying inlet/outlet width (Wi/Wo) ratios using FLOW-3D® software. The main conclusions of the present study can be summarized as follows:

- A good agreement was found between the numerical and Li's experimental results in the hydraulic characteristics and the discharge capacity, and an average relative error of the discharge capacity was 2.96% for Wi/Wo = 1.25 as the reference model.
- The hydraulic characteristics in this study confirmed that the discharge efficiency of a modified piano key weir mainly depends on the discharge efficiency over the side crest, controlled by the flow velocity along the inlet key's channel and the local submergence depth at the upstream apex of outlet keys.
- For the modified piano key weir with a ratio L/W = 5, a rounded nose and a parapet wall, the increase of the ratio between the inlet and outlet widths enables an increase in the discharge capacity of the piano key weir.
- The optimal range of Wi/Wo for maximizing discharge efficiency is within the approximate range of 1.53 - 1.67, and the best overall discharge capacity reached up to 8.5% compared with the reference model. Moreover, a ratio of Wi/Wo with Wi/Wo ≤ 1 and Wi/Wo ≥ 1.67 should be avoided in the design of the modified piano key weir in order to have a more discharge capacity.

This study provides a reference for the engineering design and practical application of the modified piano key weir. The study recommended that when designing the modifiedpiano key weir, the user should consider the range of the Wi/Wo ratio because it is significantly influenced by discharge efficiency.

Acknowledgements

This research was supported by the National Natural Science Foundation of China (Grant No. 51879227, 51279170). Ilan Ich would like to acknowledge the Chinese Scholarship Council (CSC) for hosting during his study.

Data Availability Statement

All data, models, or code generated or used during the study are available from the corresponding author by request.

Conflicts of Interest

The authors declare that they have no known competing financial interests or personal relationships that could have appeared to influence the work reported in this paper.

References

[1] Blanc, P. and Lempérière, F. (2001) Labyrinth Spillways Have a Promising Future. *International Journal on Hydropower & Dams*, **8**, 129-131.

[2] Lempérière, F. and Ouamane, A. (2003) The Piano Keys Weir: A New Cost-Effective Solution for Spillways. *International Journal on Hydropower & Dams*, **10**, 144-149.

[3] Anderson, R.M. and Tullis, B.P. (2013) Piano Key Weir Hydraulics and Labyrinth Weir Comparison. *Journal of Irrigation and Drainage Engineering*, **139**, 246-253. https://doi.org/10.1061/(ASCE)IR.1943-4774.0000530

[4] Ribeiro, M.L., Bieri, M., Boillat, J.-L., Schleiss, A., Singhal, G. and Sharma, N. (2012) Discharge Capacity of Piano Key Weirs. *Journal of Hydraulic Engineering*, **138**, 199-203. https://doi.org/10.1061/(ASCE)HY.1943-7900.0000490

[5] Pralong, J., Vermeulen, J., Blancher, B., Laugier, F., Erpicum, S., Machiels, O., Pirotton, M., Boillat, J.-L., Leite Ribeiro, M. and Schleiss, A. (2011) A Naming Convention for the Piano Key Weirs Geometrical Parameters. *Proceedings of the International Conference Labyrinth and Piano Key Weirs*, Liège, 9-11 February 2011, 271-278.

[6] Crookston, B.M., Erpicum, S., Tullis, B.P. and Laugier, F. (2019) Hydraulics of Labyrinth and Piano Key Weirs: 100 Years of Prototype Structures, Advancements, and Future Research Needs. *Journal of Hydraulic Engineering*, **145**, Article ID: 02519004. https://doi.org/10.1061/(ASCE)HY.1943-7900.0001646

[7] Chero, E., Torabi, M., Zahabi, H., Ghafoorisadatieh, A. and Bina, K. (2019) Numerical Analysis of the Circular Settling Tank. *Drinking Water Engineering and Science*, **12**, 39-44. https://doi.org/10.5194/dwes-12-39-2019

[8] Crookston, B.M., Anderson, R.M. and Tullis, B.P. (2018) Free-Flow Discharge Estimation Method for Piano Key Weir Geometries. *Journal of Hydro-Environment Research*, **19**, 160-167. https://doi.org/10.1016/j.jher.2017.10.003

[9] Koken, M., Aydin, I. and Ademoglu, S. (2022) An Iterative Hydraulic Design Methodology Based on Numerical Modeling for Piano Key Weirs. *Journal of Hydro-Environment Research*, **40**, 131-141. https://doi.org/10.1016/j.jher.2022.01.002

[10] Li, G., Li, S. and Hu, Y. (2020) The Effect of the Inlet/Outlet width Ratio on the Discharge of Piano Key Weirs. *Journal of Hydraulic Research*, **58**, 594-604. https://doi.org/10.1080/00221686.2019.1647884

[11] Li, S., Li, G., Jiang, D. and Ning, J. (2020) Influence of Auxiliary Geometric Parameters on Discharge Capacity of Piano Key Weirs. *Flow Measurement and Instrumentation*, **72**, Article ID: 101719. https://doi.org/10.1016/j.flowmeasinst.2020.101719

[12] Machiels, O., Pirotton, M., Pierre, A., Dewals, B. and Erpicum, S. (2014) Experimental Parametric Study and Design of Piano Key Weirs. *Journal of Hydraulic Research*, **52**, 326-335. https://doi.org/10.1080/00221686.2013.875070

[13] Erpicum, S., Archambeau, P., Pirotton, M. and Dewals, B. (2014) Geometric Parameters Influence on Piano Key Weir Hydraulic Performances. 5*th IAHR International Symposium on Hydraulic Structures*, Brisbane, 25-27 June 2014. https://doi.org/10.14264/uql.2014.31

[14] Anderson, R.M. (2011) Piano Key Weir Head Discharge Relationships. Utah State University, Logan.

[15] Ouamane, A. and Lempérière, F. (2006) Design of a New Economic Shape of Weir. In: Berga, L., *et al*., Eds., *Dams and Reservoirs, Societies and Environment in the* 21*st Century*, Taylor & Francis, London, 463-470.

[16] Ribeiro, M.L., Pfister, M., Schleiss, A.J. and Boillat, J.-L. (2012) Hydraulic Design of A-Type Piano Key Weirs. *Journal of Hydraulic Research*, **50**, 400-408. https://doi.org/10.1080/00221686.2012.695041

[17] Kabiri-Samani, A. and Javaheri, A. (2012) Discharge Coefficients for Free and Submerged Flow over Piano Key Weirs. *Journal of Hydraulic Research*, **50**, 114-120. https://doi.org/10.1080/00221686.2011.647888

[18] Lempérière, F. (2011) New Labyrinth Weirs Triple the Spillways Discharge. *Water and Eenrgy International*, **68**, 77-78.

[19] Lempérière, F., Vigny, J.-P. and Ouamane, A. (2011) General Comments on Labyrinth and Piano Key Weirs: The Past and Present. In: Erpicum, S., *et al*., Eds., *Labyrinth and Piano Key Weirs—PKW* 2011, Taylor & Francis, London, 17-24.

[20] Machiels, O., Erpicum, S., Dewals, B.J., Archambeau, P. and Pirotton, M. (2011) Experimental Observation of Flow Characteristics over a Piano Key Weir. *Journal of Hydraulic Research*, **49**, 359-366. https://doi.org/10.1080/00221686.2011.567761

[21] Li, S., Li, G., Miao, Z. and Chen, G. (2016) [Numerical Simulation Study on the Discharge Characteristics of a Piano Key Weir with Various Heights]. *Water Resources and Hydropower Engineering*, **47**, 60-64. (In Chinese)

[22] Lefebvre, V., Vermeulen, J. and Blancher, B. (2013) Influence of Geometrical Parameters on PK-Weirs Discharge with 3D Numerical Analysis. In: Erpicum, S., *et al*., Eds., *Labyrinth and Piano Key Weirs II—PKW* 2013, Taylor & Francis, London, 49-56.

[23] Bremer, F.L. and Oertel, M. (2017) Numerical Investigation of Wall Thickness Influence on Piano Key Weir Discharge Coefficients: A Preliminary Study. In: Erpicum, S., Laugier, F., Khanh, M.H.T. and Pfister, M., Eds., *Labyrinth and Piano Key Weirs III*, CRC Press, London, 101-108. https://doi.org/10.1201/9781315169064-14

[24] Laiadi, A., Athmani, B., Belaabed, F. and Ouamane, A. (2017) The Effect of the Geometric Shape of the Alveoli on the Performance of Piano Key Weirs. In: Erpicum, S., Laugier, F., Khanh, M.H.T. and Pfister, M., Eds., *Labyrinth and Piano Key Weirs III*, CRC Press, London, 93-100. https://doi.org/10.1201/9781315169064-13

[25] Li, S. (2020) [Study on Hydraulic Characteristics and Geometric Parameters of Piano Key Weir]. Xi'an University of Technology, Xian.

[26] Anderson, R.M. and Tullis, B.P. (2012) Comparison of Piano Key and Rectangular Labyrinth Weir Hydraulics. *Journal of Hydraulic Engineering*, **138**, 358-361. https://doi.org/10.1061/(ASCE)HY.1943-7900.0000509

[27] Sangsefidi, Y., Mehraein, M. and Ghodsian, M. (2015) Numerical Simulation of Flow over Labyrinth Spillways. *Scientia Iranica*, **22**, 1779-1787.

[28] Safarzadeh, A. and Noroozi, B. (2017) 3D Hydrodynamics of Trapezoidal Piano Key Spillways. *International Journal of Civil Engineering*, **15**, 89-101. https://doi.org/10.1007/s40999-016-0100-8

[29] Chahartaghi, M.K., Nazari, S. and Shooshtari, M.M. (2019) Experimental and Numerical Simulation of Arced Trapezoidal Piano Key Weirs. *Flow Measurement and Instrumentation*, **68**, Article ID: 101576. https://doi.org/10.1016/j.flowmeasinst.2019.101576

[30] Ghanbari, R. and Heidarnejad, M. (2020) Experimental and Numerical Analysis of Flow Hydraulics in Triangular and Rectangular Piano Key Weirs. *Water Science*, **34**, 32-38. https://doi.org/10.1080/11104929.2020.1724649

[31] Li, S., Li, G. and Jiang, D. (2020) Physical and Numerical Modeling of the Hydraulic Characteristics of Type-A Piano Key Weirs. *Journal of Hydraulic Engineering*, **146**, 06020004. https://doi.org/10.1061/(ASCE)HY.1943-7900.0001716

[32] FLOW-3D (2016) FLOW-3D® Version 11.2 Users Manual. FLOW-3D [Computer Software]. Flow Science, Inc., Santa Fe. https://www.flow3d.com

[33] Hirt, C.W. and Nichols, B.D. (1981) Volume of Fluid (VOF) Method for the Dynamics of Free Boundaries. *Journal of Computational Physics*, **39**, 201-225. https://doi.org/10.1016/0021-9991(81)90145-5

[34] Abbasi, S., Fatemi, S., Ghaderi, A. and Di Francesco, S. (2020) The Effect of Geometric Parameters of the Antivortex on a Triangular Labyrinth Side Weir. *Water*, **13**, Article No. 14. https://doi.org/10.3390/w13010014

[35] Ghaderi, A., Daneshfaraz, R., Abbasi, S. and Abraham, J. (2020) Numerical Analysis of the Hydraulic Characteristics of Modified Labyrinth Weirs. *International Journal of Energy and Water Resources*, **4**, 425-436. https://doi.org/10.1007/s42108-020-00082-5

[36] Roache, P.J. (1994) Perspective: A Method for Uniform Reporting of Grid Refinement Studies. *Journal of Fluids Engineering*, **116**, 405-413. https://doi.org/10.1115/1.2910291

[37] Sicilian, J.M., Hirt, C.W. and Harper, R.P. (1987) FLOW-3D. Computational Modeling Power for Scientists and Engineers. Report FSI-87-00-1. Flow Science, Los Alamos.

[38] Gharahjeh, S., Aydin, I. and Altan-Sakarya, A.B. (2015) Weir Velocity Formulation for Sharp-Crested Rectangular Weirs. *Flow Measurement and Instrumentation*, **41**, 50-56. https://doi.org/10.1016/j.flowmeasinst.2014.10.018

[39] Hager, W.H. and Schleiss, A.J. (2009) Constructions Hydrauliques: Ecoulements Stationnaires. Presses Polytechniques et Universitaires Romandes, Lausanne.

[40] Zech, Y. (2010) Constructions Hydrauliques: Ecoulements Stationnaires [Hydraulic Structures—Steady Flows]. *Journal of Hydraulic Research*, **48**, 555-556. https://doi.org/10.1080/00221686.2010.492096

[41] Machiels, O. (2012) Experimental Study of the Hydraulic Behaviour of Piano Key Weirs. Université de Liège, Liège, Belgium.

[42] Machiels, O., Erpicum, S., Archambeau, P., Dewals, B. and Pirotton, M. (2013) Parapet Wall Effect on Piano Key Weir Efficiency. *Journal of Irrigation and Drainage Engineering*, **139**, 506-511. https://doi.org/10.1061/(ASCE)IR.1943-4774.0000566

[43] Ribeiro, M.L., Bieri, M., Boillat, J.-L., Schleiss, A.J., Delorme, F. and Laugier, F. (2009) Hydraulic Capacity Improvement of Existing Spillways: Design of Piano Key Weirs. *Vingt Troisieme Congres Des Grands Barrages Brasilia*, Brasília, Brazil, May 2009.